
MetaPerturb: Transferable Regularizer for Heterogeneous Tasks and Architectures

Jeongun Ryu^{1*} Jaewoong Shin^{1*} Hae Beom Lee^{1*} Sung Ju Hwang^{1,2}
¹KAIST, ²AITRICS, South Korea
{rjw0205, shinjw148, haebeom.lee, sjhwang82}@kaist.ac.kr

Abstract

Regularization and transfer learning are two popular techniques to enhance model generalization on unseen data, which is a fundamental problem of machine learning. Regularization techniques are versatile, as they are task- and architecture-agnostic, but they do not exploit a large amount of data available. Transfer learning methods learn to transfer knowledge from one domain to another, but may not generalize across tasks and architectures, and may introduce new training cost for adapting to the target task. To bridge the gap between the two, we propose a transferable perturbation, *MetaPerturb*, which is meta-learned to improve generalization performance on unseen data. *MetaPerturb* is implemented as a set-based lightweight network that is agnostic to the size and the order of the input, which is shared across the layers. Then, we propose a meta-learning framework, to jointly train the perturbation function over heterogeneous tasks in parallel. As *MetaPerturb* is a set-function trained over diverse distributions across layers and tasks, it can generalize to heterogeneous tasks and architectures. We validate the efficacy and generality of *MetaPerturb* trained on a specific source domain and architecture, by applying it to the training of diverse neural architectures on heterogeneous target datasets against various regularizers and fine-tuning. The results show that the networks trained with *MetaPerturb* significantly outperform the baselines on most of the tasks and architectures, with a negligible increase in the parameter size and no hyperparameters to tune.

1 Introduction

The success of Deep Neural Networks (DNNs) largely owes to their ability to accurately represent arbitrarily complex functions. However, at the same time, the excessive number of parameters, which enables such expressive power, renders them susceptible to overfitting especially when we do not have a sufficient amount of data to ensure generalization. There are two popular techniques that can help with generalization of deep neural networks: transfer learning and regularization.

Transfer learning [39] methods aim to overcome this data scarcity problem by transferring knowledge obtained from a source dataset to effectively guide the learning on the target task. Whereas the existing transfer learning methods have been proven to be very effective, there also exist some limitations. Firstly, their performance gain highly depends on the similarity between source and target domains, and knowledge transfer across different domains may not be effective or even degenerate the performance on the target task. Secondly, many transfer learning methods require the neural architectures for the source and the target tasks to be the same, as in the case of fine-tuning. Moreover, transfer learning methods usually require additional memory and computational cost for knowledge transfer. Many require to store the entire set of parameters for the source network (e.g. fine-tuning, LwF [21], attention transfer [47]), and some methods require extra training to transfer the source

*: Equal contribution

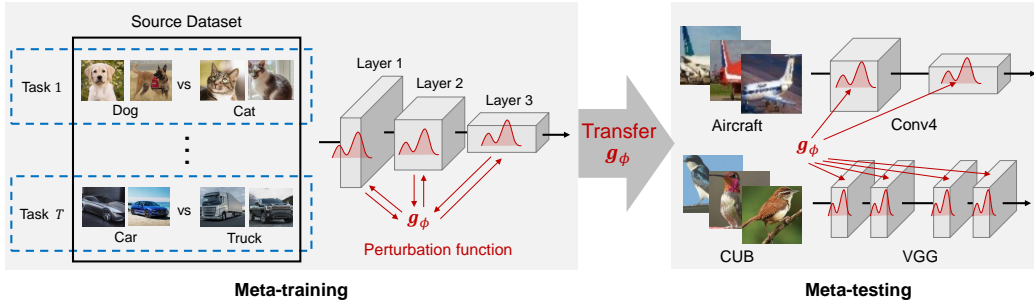


Figure 1: **Concepts.** We learn our perturbation function at meta-training stage and use it to solve diverse meta-testing tasks that come with diverse network architectures.

knowledge to the target task [14]. Such restriction makes transfer learning unappealing, and thus not many of them are used in practice except for simple fine-tuning of the networks pre-trained on large datasets (e.g. convolutional networks pretrained on ImageNet [33], BERT [7] trained on Wikipedia).

On the other hand, regularization techniques, which leverage human prior knowledge on the learning tasks to help with generalization, are more versatile as they are domain- and architecture- agnostic. Penalizing the ℓ_p -norm of the weights [28], dropping out random units or filters [10, 38], normalizing the distribution of latent features at each input [13, 41, 45], randomly mixing or perturbing samples [42, 50], are instances of such domain-agnostic regularizations. They are more favored in practice over transfer learning since they can work with any architectures and do not incur extra memory or computational overhead, which is often costly with many advanced transfer learning techniques. However, regularization techniques are limited in that they do not exploit the rich information in the large amount of data available.

These limitations of transfer learning and regularization techniques motivate us to come up with a *transferable regularization* technique that can bridge the gap between the two different approaches for enhancing generalization. Such a transferable regularizer should learn useful knowledge from the source task for regularization, while generalizing across different domains and architectures, with minimal extra cost. A recent work [19] propose to meta-learn a noise generator for few-shot learning, to improve the generalization on unseen tasks. Yet, the proposed gradient-based meta-learning scheme cannot scale to standard learning settings which require large amount of steps to converge to good solutions and is inapplicable to architectures that are different from the source network architecture.

To overcome these difficulties, we propose a novel lightweight, scalable perturbation function that is *meta-learned* to improve generalization on unseen tasks and architectures for standard training (See Figure 1 for the concept). Our model generates regularizing perturbations to latent features, given the set of original latent features at each layer. Since it is implemented as an order-equivariant set function, it can be shared across layers and networks learned with different initializations. We meta-learn our perturbation function by a simple joint training over multiple subsets of the source dataset in parallel, which largely reduces the computational cost of meta-learning.

We validate the efficacy and efficiency of our transferable regularizer *MetaPerturb* by training it on a specific source dataset and applying the learned function to the training of heterogeneous architectures on a large number of datasets with varying degrees of task similarity. The results show that networks trained with our meta regularizer outperforms recent regularization techniques and fine-tuning, and obtains significantly improved performances even on largely different tasks on which fine-tuning fails. Also, since the optimal amount of perturbation is automatically learned at each layer, *MetaPerturb* does not have any hyperparameters unlike most of the existing regularizers. Such effectiveness, efficiency, and versatility of our method makes it an appealing transferable regularization technique that can replace or accompany fine-tuning and conventional regularization techniques.

The contribution of this paper is threefold:

- We propose a lightweight and versatile perturbation function that can transfer the knowledge of a source task to heterogeneous target tasks and architectures.
- We propose a novel meta-learning framework in the form of joint training, which allows to efficiently perform meta-learning on large-scale datasets in the standard learning framework.
- We validate our perturbation function on a large number of datasets and architectures, on which it successfully outperforms existing regularizers and finetuning.

2 Related Work

Transfer Learning Transfer learning [39] is one of the popular tools in deep learning to solve the data scarcity problem. The most widely used method in transfer learning is fine-tuning [34] which first trains parameters in the source domain and then use them as the initial weights when learning for the target domain. ImageNet [33] pre-trained network weights are widely used for fine-tuning, achieving impressive performance on various computer vision tasks (e.g. semantic segmentation [22], object detection [11]). However, if the source and target domain are semantically different, fine-tuning may result in negative transfer [46]. Further it is inapplicable when the target network architecture is different from that of the source network. Transfer learning frameworks often require extensive hyperparameter tuning (e.g. which layers to transfer, fine-tuning or not, etc). Recently, Jang et al. [14] proposed a framework to overcome this limitation which can automatically learn what knowledge to transfer from the source network and between which layer to perform knowledge transfer. However, it requires large amount of additional training for knowledge transfer, which limits its practicality. Most of the existing transfer learning methods aim to transfer the features themselves, which may result in negative or zero transfer when the source and the target domains are dissimilar. Contrary to existing frameworks, our framework transfers how to perturb the features in the latent space, which can yield performance gains even on domain-dissimilar tasks.

Regularization methods Training with our input-dependent perturbation function is reminiscent of some of existing input-dependent regularizers. Specifically, information bottleneck methods [40] with variational inference have input-dependent form of perturbation function applied to both training and testing examples as with ours. Variational Information Bottleneck [2] introduces additive noise whereas Information Dropout [1] applies multiplicative noise as with ours. The critical difference from those existing regularizers is that our perturbation function is meta-learned while they do not involve such knowledge transfer. A recently proposed meta-regularizer, Meta Dropout [19] is relevant to ours as it learns to perturb the latent features of training examples for generalization. However, it specifically targets for meta-level generalization in few-shot meta-learning, and does not scale to standard learning frameworks with large number of inner gradient steps as it runs on the MAML framework [8] that requires lookahead gradient steps. Meta Dropout also requires the noise generator to have the same architecture as the source network, which limits its practicality with large networks and makes it impossible to generalize over heterogeneous architectures.

Meta Learning Our regularizer is meta-learned to generalize over heterogeneous tasks and architectures. Meta-learning [13] aims to learn common knowledge that can be shared over distribution of tasks, such that the model can generalize to unseen tasks. While the literature on meta-learning is vast, we name a few works that are most relevant to ours. Finn et al. [8] proposes a model-agnostic meta-learning (MAML) framework to find a shared initialization parameter that can be fine-tuned to obtain good performance on an unseen target task a few gradient steps. The main difficulty is that the number of inner-gradient steps is excessively large for standard learning scenarios, when compared to few-shot learning cases. This led the follow-up works to focus on reducing the computational cost of extending the inner-gradient steps [3, 9, 29, 31], but still they assume we take at most hundreds of gradient steps from a shared initialization. On the other hand, Ren et al. [32] and its variant [35] propose to use an online approximation of the full inner-gradient steps, such that we lookahead only a single gradient step and the meta-parameter is optimized with the main network parameter at the same time in an online manner. While effective for standard learning, they are still computationally inefficient due to the expensive bi-level optimization. As an approach to combine meta-learning with regularization, MetaMixup [24] meta-learns the hyperparameter of Mixup and MetaReg [5] proposes to meta-learn the regularization parameter (ℓ_1 for domain generalization), but they consider generalization within a single task or across similar domains, while ours target heterogeneous domains. Differently from all existing meta-learning approaches, by resorting to simple joint training on fixed subsets of the dataset, we efficiently extend the meta-learning framework from few-shot learning into a standard learning frameworks for transfer learning.

3 Approach

In this section, we introduce our perturbation function that is applicable to any convolutional network architectures and to any image datasets. We then further explain our meta-learning framework for efficiently learning the proposed perturbation function in the standard learning framework.

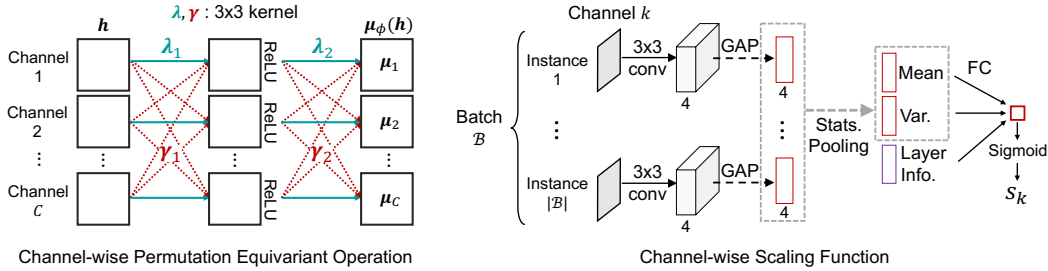


Figure 2: **Left:** The architecture of the channel-wise permutation equivariant operation. **Right:** The architecture of the channel-wise scaling function taking a batch of instances as an input.

3.1 Dataset and Network agnostic perturbation function

The conventional transfer learning method transfers the entire set or a subset of the main network parameters θ . However such parameter transfer may become ineffective when we transfer knowledge across a dissimilar pair of source and target tasks. Further, if we need to use a different neural architecture for the target task, it becomes simply inapplicable. Thus, we propose to focus on transferring another set of parameters ϕ which is disjoint from θ and is extremely light-weight. In this work, we let ϕ be the parameter for the *perturbation function* which are learned to regularize latent features of convolutional neural networks. The important assumption here is that even if a disjoint pair of source and target task requires different feature extractors for each, there may exist some general rules of perturbation that can effectively regularize both feature extractors at the same time.

Another property that we want to impose upon our perturbation function is its general applicability to any convolutional neural network architectures. The perturbation function should be applicable to:

- Neural networks with **undefined number of convolutional layers**. We can solve this problem by allowing the function to be shared across the convolutional layers.
- Convolutional layers with **undefined number of channels**. We can tackle this problem either by sharing the function across channels or using permutation-equivariant set encodings.

3.2 MetaPerturb

We now describe our novel perturbation function, *MetaPerturb* that satisfies the above requirements. It consists of the following two components: input-dependent stochastic noise generator and batch-dependent scaling function.

Input-dependent stochastic noise generator The first component is an input-dependent stochastic noise generator, which has been empirically shown by Lee et al. [19] to often outperform the input-independent counterparts. To make the noise applicable to any convolutional layers, we propose to use permutation equivariant set-encoding [49] across the channels. It allows to consider interactions between the feature maps at each layer while making the generated perturbations to be invariant to the re-orderings caused by random initializations.

Zaheer et al. [49] showed that for a linear transformation $\mu_{\phi'} : \mathbb{R}^C \rightarrow \mathbb{R}^C$ parameterized by a matrix $\phi' \in \mathbb{R}^{C \times C}$, $\mu_{\phi'}$ is permutation equivariant to the C input elements *iff* the diagonal elements of ϕ' are equal and also the off-diagonal elements of ϕ' are equal as well, i.e. $\phi' = \lambda' \mathbf{I} + \gamma' \mathbf{1}\mathbf{1}^T$ with $\lambda', \gamma' \in \mathbb{R}$ and $\mathbf{1} = [1, \dots, 1]^T$. The diagonal elements map each of the input elements to themselves, whereas the off-diagonal elements capture the interactions between the input elements.

Here, we propose an equivalent form for convolution operation, such that the output feature maps μ_ϕ are equivariant to the channel-wise permutations of the input feature maps \mathbf{h} . We assume that ϕ consists of the following two types of parameters: $\lambda \in \mathbb{R}^{3 \times 3}$ for self-to-self convolution operation and $\gamma \in \mathbb{R}^{3 \times 3}$ for all-to-self convolution operation. We then similarly combine λ and γ to produce a convolutional weight tensor of dimension $\mathbb{R}^{C \times C \times 3 \times 3}$ for C input and output channels (See Figure 2 (left)). Zaheer et al. [49] also showed that a stack of multiple permutation equivariant operations is also permutation equivariant. Thus we stack two layers of μ_ϕ with different parameters and ReLU nonlinearity in-between them in order to increase the flexibility of μ_ϕ (See Figure 2 (left)).

Finally, we sample the input-dependent stochastic noise \mathbf{z} from the following distribution:

$$\mathbf{z} = \text{Softplus}(\mathbf{a}), \quad \mathbf{a} \sim \mathcal{N}(\boldsymbol{\mu}_\phi(\mathbf{h}), \mathbf{I}) \quad (1)$$

where we fix the variance of \mathbf{a} to \mathbf{I} following Lee et al. [19] to eliminate any hyperparameters, which we empirically found to work well in practice.

Batch-dependent scaling function The next component is batch-dependent scaling function, which scales each channel to different values between $[0, 1]$ for a given batch of examples. The assumption here is that the proper amount of the usage for each channel should be adaptively decided for each dataset by using a soft multiplicative gating mechanism. In Figure 2 (right), at training time, we first collect examples in batch \mathcal{B} , apply convolutions, followed by global average pooling (GAP) for each channel k to extract 4-dimensional vector representations of the channel. We then compute statistics of them such as mean and diagonal covariance over batch and further concatenate the layer information such as the number of channels C and the width W (or equivalently, the height H) to the statistics. We finally generate the scales s_1, \dots, s_C with a shared affine transformation and a sigmoid function, and collect them into a single vector $\mathbf{s} = [s_1, \dots, s_C] \in [0, 1]^C$. At testing time, instead of using batch-wise scales, we use global scales accumulated by moving average at the training time similarly to batch normalization [13]. Although this scaling term may look similar to the feature-wise linear modulation (FiLM) [30], it is different as ours is meta-learned and performs batch-wise scaling whereas FiLM performs instance-wise scaling and is not meta-learned.

Final form We lastly combine \mathbf{z} and \mathbf{s} to obtain the following form of the perturbation $\mathbf{g}_\phi(\mathbf{h})$:

$$\mathbf{g}_\phi(\mathbf{h}) = \mathbf{s} \circ \mathbf{z} \quad (2)$$

where \circ denotes channel-wise multiplication. We then multiply $\mathbf{g}_\phi(\mathbf{h})$ back to the input feature maps \mathbf{h} , at every layer (every block for ResNet [12]) of the network (See Figure 3). We empirically verified that clipping the combined feature map values with a constant k (e.g. $k = 100$) during meta-training helps with its stability since the perturbation may excessively amplify some of the feature map values. Note that since the noise generator is shared across all the channels and layers, our transferable regularizer can perform knowledge transfer with marginal parameter overhead (e.g. 82). Further, there is no hyperparameter to tune², since the proper amount of the two perturbations is meta-learned and automatically decided for each layer and channel.

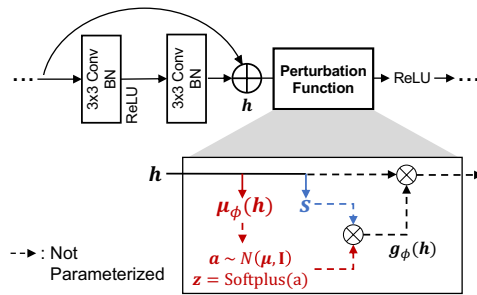


Figure 3: **The architecture of our perturbation function** applicable to any convolutional neural networks (e.g. ResNet)

3.3 Meta-learning framework

The next important question is how to efficiently meta-learn the parameter ϕ for the perturbation function. There are two challenges: **1)** Because of the large size of each source task, it is costly to sequentially alternate between the tasks within a single GPU, unlike few-shot learning where each task is sufficiently small. **2)** The computational cost of lookahead operation and second-order derivative in online approximation proposed by Ren et al. [32] is still too expensive.

Distributed meta-learning To solve the first problem, we class-wisely divide the source dataset to generate T (e.g. 10) tasks with *fixed* samples and distribute them across multiple GPUs for parallel learning of the tasks. Then, throughout the entire meta-training phase, we only need to share the low-dimensional (e.g. 82) meta parameter ϕ between the GPUs without sequential alternating training over the tasks. Such a way of meta-learning is simple yet novel, and scalable to the number of tasks when a sufficient number of GPUs are available.

²The feature map clipping value, k , need not be tuned and the clipping could be simply omitted.

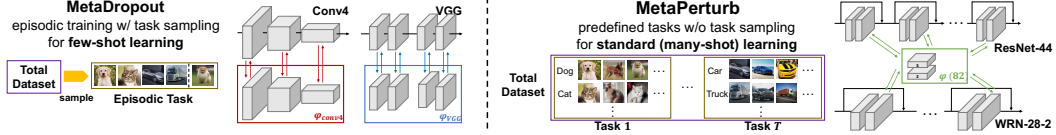


Figure 4: **Comparison with MetaDropout [19]**. While MetaDropout also meta-learns a noise generator, it is tied to a specific architecture and cannot scale to large networks and datasets since it learns a different noise generator at each layer and uses MAML, which is not scalable.

Algorithm 1 Meta-training	Algorithm 2 Meta-testing
1: Input: $(\mathcal{D}_1^{\text{tr}}, \mathcal{D}_1^{\text{te}}), \dots, (\mathcal{D}_T^{\text{tr}}, \mathcal{D}_T^{\text{te}})$	1: Input: $\mathcal{D}^{\text{tr}}, \mathcal{D}^{\text{te}}, \phi^*$
2: Input: Learning rate α	2: Input: Learning rate α
3: Output: ϕ^*	3: Output: θ^*
4: Randomly initialize $\theta_1, \dots, \theta_T, \phi$	4: Randomly initialize θ
5: while not converged do	5: while not converged do
6: for $t = 1$ to T do	6: Sample $\mathcal{B}_t^{\text{tr}} \subset \mathcal{D}_t^{\text{tr}}$.
7: Sample $\mathcal{B}_t^{\text{tr}} \subset \mathcal{D}_t^{\text{tr}}$ and $\mathcal{B}_t^{\text{te}} \subset \mathcal{D}_t^{\text{te}}$.	7: Compute $\mathcal{L}(\mathcal{B}_t^{\text{tr}}; \theta, \phi^*)$ w/ perturbation.
8: Compute $\mathcal{L}(\mathcal{B}_t^{\text{tr}}; \theta_t, \phi)$ w/ perturbation.	8: $\theta \leftarrow \theta - \alpha \nabla_{\theta} \mathcal{L}(\mathcal{B}_t^{\text{tr}}; \theta, \phi^*)$
9: $\theta_t \leftarrow \theta_t - \alpha \nabla_{\theta_t} \mathcal{L}(\mathcal{B}_t^{\text{tr}}; \theta_t, \phi)$	9: end while
10: Compute $\mathcal{L}(\mathcal{B}_t^{\text{te}}; \theta_t, \phi)$ w/ perturbation.	10: Evaluate the test examples in \mathcal{D}^{te} with MC approximation and the parameter θ^* .
11: end for	11:
12: $\phi \leftarrow \phi - \alpha \nabla_{\phi} \frac{1}{T} \sum_{t=1}^T \mathcal{L}(\mathcal{B}_t^{\text{te}}; \theta_t, \phi)$	12:
13: end while	

Knowledge transfer at the limit of convergence To solve the second problem, we propose to further approximate the online approximation [32] by simply ignoring the bi-level optimization and the corresponding second-order derivative. It means we simply focus on knowledge transfer across the tasks *only at the limit of the convergence* of the tasks. Toward this goal, we propose to perform a joint optimization of $\theta = \{\theta_1, \dots, \theta_T\}$ and ϕ , each of which maximizes the log likelihood of the training dataset \mathcal{D}^{tr} and test dataset \mathcal{D}^{te} , respectively:

$$\phi^*, \theta^* = \operatorname{argmax}_{\phi, \theta} \sum_{t=1}^T \left\{ \log p(\mathbf{y}_t^{\text{te}} | \mathbf{X}_t^{\text{te}}; \text{StopGrad}(\theta_t), \phi) + \log p(\mathbf{y}_t^{\text{tr}} | \mathbf{X}_t^{\text{tr}}; \theta_t, \text{StopGrad}(\phi)) \right\} \quad (3)$$

where $\text{StopGrad}(x)$ denotes that we do not compute the gradient and consider x as constant. See the Algorithm 1 and 2 for meta-training and meta-test, respectively. The intuition is that, even with this naive approximation, the final ϕ^* will be transferable if we confine the limit of transfer to *around the convergence*, since we know that ϕ^* already has satisfied the desired property at the end of the convergence of multiple meta-training tasks, i.e. over $\theta_1^*, \dots, \theta_T^*$. It is natural to expect similar consequence at meta-test time if we let the novel task $T + 1$ jointly converge with the meta-learned ϕ^* to obtain θ_{T+1}^* . We empirically verified that this simple joint meta-learning suffers from negligible accuracy loss over meta-learning with a single lookahead step [32], while achieving order of magnitude faster training time depending on the tasks and architectures. Further, gradually increasing the strength of our perturbation function \mathbf{g}_{ϕ} performs much better than without such annealing, which means that the knowledge transfer may be less effective at the early stage of the training, but becomes more effective at later steps, i.e. near the convergence. We can largely reduce the computational cost of meta-training with this naive approximation.

Comparison with MetaDropout MetaDropout [19] also proposes to meta-learn the noise generator. However, it is largely different from MetaPerturb in multiple aspects. First of all, MetaDropout cannot generalize across heterogeneous neural architectures, since it learns an individual noise generator for each layer (Figure 2 of [19]). Thus it is tied to the specific base network architecture (Fig 4), while MetaPerturb can generalize across architectures. Moreover, MetaDropout does not scale to large networks since the noise generator should be the same size as the main network. MetaPerturb, on the other hand, requires marginal parameter overhead (82) even for deep CNNs since it shares the same lightweight noise generator across all layers and channels. MetaDropout also cannot scale to standard learning with large number of instance and deep networks (Fig 4), since it uses episodic training and MAML for meta-learning. We overcome such a challenge with a scalable distributed joint meta-learning framework described in the earlier paragraphs.

Table 1: **Transfer to multiple datasets.** We use ResNet 20 as the source and target networks. TIN denotes the Tiny ImageNet dataset. The reported results are mean accuracies and standard deviations over 5 meta-test runs.

Model	# Transfer params	Source dataset	Target Dataset					
			STL10	s-CIFAR100	Dogs	Cars	Aircraft	CUB
Base	0	None	66.78±0.59	31.79±0.24	34.65±1.05	44.34±1.10	59.23±0.95	30.63±0.66
Info. Dropout [1]	0	None	67.46±0.17	32.32±0.33	34.63±0.68	43.13±2.31	58.59±0.90	30.83±0.79
DropBlock [10]	0	None	68.51±0.67	32.74±0.36	34.59±0.87	45.11±1.47	59.76±1.38	30.55±0.26
Manifold Mixup [42]	0	None	72.83±0.69	39.06±0.73	36.29±0.70	48.97±1.69	64.35±1.23	37.80±0.53
MetaPerturb	82	TIN	69.98±0.63	34.57±0.38	38.41±0.74	62.46±0.80	65.87±0.77	42.01±0.43
Finetuning (FT)	.3M	TIN	77.16±0.41	43.69±0.22	40.09±0.31	58.61±1.16	66.03±0.85	34.89±0.30
FT + Info. Dropout	.3M + 0	TIN	77.41±0.13	43.92±0.44	40.04±0.46	58.07±0.57	65.47±0.27	35.55±0.81
FT + DropBlock	.3M + 0	TIN	78.32±0.31	44.84±0.37	40.54±0.56	61.08±0.61	66.30±0.84	34.61±0.54
FT + Manif. Mixup	.3M + 0	TIN	79.60±0.27	47.92±0.79	42.54±0.70	64.81±0.97	71.53±0.80	43.07±0.83
FT + MetaPerturb	.3M + 82	TIN	78.27±0.36	47.41±0.40	46.06±0.44	73.04±0.45	72.34±0.41	48.60±1.14

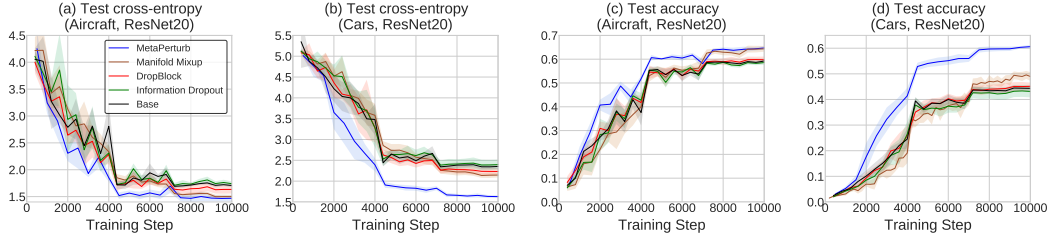


Figure 5: **Convergence plots** on Aircraft [25] and Stanford Cars [16] datasets.

4 Experiments

We next validate our method under realistic learning scenarios where target tasks can come with arbitrary image datasets and arbitrary convolutional network architectures. For the base regularizations, we used the weight decay of 0.0005 and random cropping and horizontal flipping in all experiments.

4.1 Transfer to multiple datasets

We first validate if our meta-learned perturbation function can generalize to multiple target datasets.

Datasets We use **Tiny ImageNet** [18] as the source dataset, which is a subset of the ImageNet [33] dataset. It consists of 64×64 size images from 200 classes, with 500 training images for each class. We class-wisely split the dataset into 10 splits to produce heterogeneous task samples. We then transfer our perturbation function to the following target tasks: **STL10** [6], **CIFAR-100** [17], **Stanford Dogs** [15], **Stanford Cars** [16], **Aircraft** [25], and **CUB** [44]. STL10 and CIFAR-100 are benchmark classification datasets of general categories, which is similar to the source dataset. Other datasets are for fine-grained classification, and thus quite dissimilar from the source dataset. We resize the images of the fine-grained classification datasets into 84×84 . Lastly, for CIFAR-100, we sub-sample 5,000 images from the original training set in order to simulate data-scarce scenario (i.e. prefix *s*-). See the Appendix for more detailed information for the datasets.

Baselines and our model We consider the following well-known stochastic regularizers to compare our model with. We carefully tuned the hyperparameters of each baseline with a holdout validation set for each dataset. Note that MetaPerturb does not have any hyperparameters to tune, but there could be variations among runs as with any neural models. Thus we select the best performing noise generator over five meta-training runs using a validation set consisting of samples from CIFAR-100, that is disjoint from *s*-CIFAR100, and use it throughout all the experiments in the paper. **Information Dropout:** This model [1] is an instance of Information Bottleneck (IB) method [40], where the bottleneck variable is defined as multiplicative perturbation as with ours. **DropBlock:** This model [10] is a type of structured dropout [38] specifically developed for convolutional networks, which randomly drops out units in a contiguous region of a feature map together. **Manifold Mixup:** A recently introduced stochastic regularizer [42] that randomly pairs training examples to linearly interpolate between the latent features of them. We also compare with **Base** and **Finetuning** which have no regularizer added.

Results Table 1 shows that our MetaPerturb regularizer significantly outperforms all the baselines on most of the datasets with only 82 dimensions of parameters transferred. MetaPerturb is especially effective on the fine-grained datasets. This is because the generated perturbations help focus on

Table 2: **Transfer to multiple networks.** We use Tiny ImageNet as the source and small-SVHN as the target dataset. As for Finetuning, we use the same source and target network since it cannot be applied across two different networks. The reported numbers are the mean accuracies and standard deviations over 5 meta-test runs.

Model	Source Network	Target Network					
		Conv4	Conv6	VGG9	ResNet20	ResNet44	WRN-28-2
Base	None	83.93±0.20	86.14±0.23	88.44±0.29	87.96±0.30	88.94±0.41	88.95±0.44
Information Dropout	None	84.91±0.34	87.23±0.26	88.29±1.18	88.46±0.65	89.33±0.20	89.51±0.29
DropBlock	None	84.29±0.24	86.22±0.26	88.68±0.35	89.43±0.26	90.14±0.18	90.55±0.25
Finetuning	Same	84.00±0.27	86.56±0.23	88.17±0.18	88.77±0.26	89.62±0.05	89.85±0.31
MetaPerturb	ResNet20	86.61±0.42	88.59±0.26	90.24±0.27	90.70±0.25	90.97±1.09	90.88±0.07

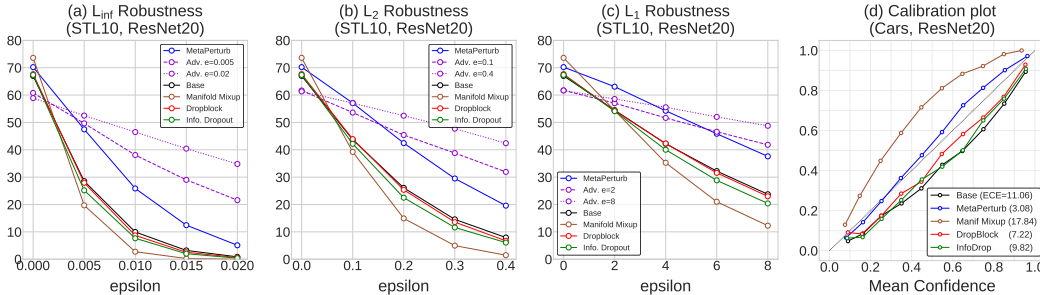


Figure 6: (a-c) Adversarial robustness against EoT attacks with varying size of radius ϵ . (d) Calibration plot.

relevant part of the input by injecting noise \mathbf{z} or downweighting the scale \mathbf{s} of the distracting parts of the input. Our model also outperforms the baselines with significant margins when used along with finetuning (on Tiny ImageNet dataset). All these results demonstrate that our model can effectively regularize the networks trained on unseen tasks from heterogeneous task distributions. Figure 5 shows that MetaPerturb achieves better convergence over the baselines in terms of test loss and accuracy.

4.2 Transfer to multiple networks

We next validate if our meta-learned perturbation can generalize to multiple network architectures.

Dataset and Networks We use small version of SVHN dataset [27] (total 5,000 instances). We use networks with 4 or 6 convolutional layers with 64 channels (Conv4 [43] and Conv6), VGG9 (a small version of VGG [37] used in [36]), ResNet20, ResNet44 [12] and Wide ResNet 28-2 [48].

Results Table 2 shows that our MetaPerturb regularizer significantly outperforms the baselines on all the network architectures we considered. Note that although the source network is fixed as ResNet20 during meta-training, the statistics of the layers are very diverse, such that the shared perturbation function is learned to generalize over diverse input statistics. We conjecture that such sharing across layers is the reason MetaPerturb effectively generalize to diverse target networks. While finetuning generally outperforms learning from scratch in most cases, for experiments with SVHN which contains digits and which is largely different from classes in TIN (Table 2), the performance gain becomes smaller. Contrarily, MetaPerturb obtains large performance gains even on heterogeneous datasets, which shows that the knowledge of how to perturb a sample is more generic and is applicable to diverse domains.

4.3 Adversarial robustness and calibration performance

Reliability Figure 6(a) shows that MetaPerturb achieves higher robustness over existing baselines against *Expectation over Time* (EoT) [4] PGD attacks without explicit adversarial training, and even higher robust accuracy over adversarial training [23] against ℓ_2 and ℓ_1 attacks with small amount of perturbations. Figure 6(d) shows that our MetaPerturb also improves the calibration performance in terms of the expected calibration error (ECE [26]) and calibration plot, while other regularizers do not, and Manifold Mixup even yields worse calibration over the base model.

Qualitative analysis Figure 7 shows the learned scale \mathbf{s} across the layers for each dataset. We see that \mathbf{s} for each channel and layer are generated differently for each dataset. The amount of channel scaling at the lower layers have low variance across the channels and datasets which may be because they are generic features of almost equal importance. Contrarily, the amount of perturbations at the upper layers are highly variable across channels and datasets, since the scaling term \mathbf{s} modulates the amount of noise differently for each channel according to their (noises’) relevance to the given task.

Table 3: Ablation study.

Variants			s-CIFAR100	Aircraft	CUB
Base			31.79±0.24	59.23±0.95	30.63±0.66
(a)	Components of perturbation	w/o channel-wise scaling s	32.65±0.40	63.56±1.30	33.63±0.92
		w/o stochastic noise \mathbf{z}	31.02±0.44	58.32±0.92	30.26±0.67
(b)	Location of perturbation	Only before pooling	32.89±0.33	61.39±1.01	38.88±1.15
		Only at top layers	32.57±0.46	57.51±0.72	37.89±0.58
		Only at bottom layers	31.77±0.42	61.32±0.29	33.48±0.57
(c)	Meta-training strategy	Homogeneous task distribution	34.31±0.88	65.41±0.76	40.64±0.31
		MetaPerturb	34.47±0.45	65.87±0.77	42.01±0.43

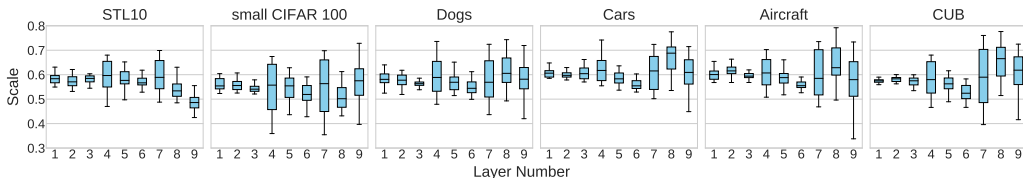


Figure 7: The scale s at each block of ResNet20.

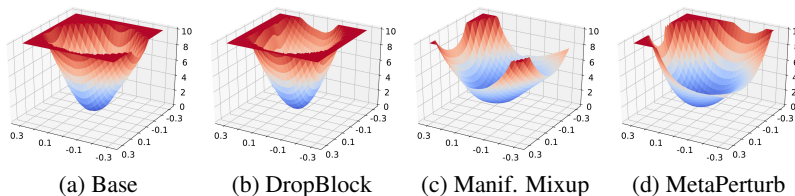


Figure 8: Visualization of training loss surface [20] (CUB, ResNet20)

Figure 8 shows that models trained with MetaPerturb and Manifold Mixup have flatter loss surfaces than the baselines’, which may be a reason why MetaPerturb improves model generalization.

Ablation study (a) Components of the perturbation function: In Table 3(a), we can see that both components of our perturbation function, the input-dependent stochastic noise \mathbf{z} and the channel-wise scaling s jointly contribute to the good performance of our MetaPerturb regularizer.

(b) Location of the perturbation function: Also, in order to find appropriate location of the perturbation function, we tried applying it to various parts of the networks in Table 3(b) (e.g. only before pooling layers or only at top/bottom layers). We can see that applying the function to a smaller subset of layers largely underperforms applying it to all the ResNet blocks as done with MetaPerturb.

(c) Source task distribution: Lastly, in order to verify the importance of heterogeneous task distribution, we compare with the homogeneous task distribution by splitting the source dataset across the instances, rather than across the classes as done with MetaPerturb. We observe that this strategy results in performance degradation since the lack of diversity prevents the perturbation function from effectively extrapolating to diverse tasks.

5 Conclusion

We proposed a light-weight perturbation function that can transfer the knowledge of a source task to any convolutional architectures and image datasets, by bridging the gap between regularization methods and transfer learning. This is done by implementing the noise generator as a permutation-equivariant set function that is shared across different layers of deep neural networks, and meta-learning it. To scale up meta-learning to standard learning frameworks, we proposed a simple yet effective meta-learning approach, which divides the dataset into multiple subsets and train the noise generator jointly over the subsets, to regularize networks with different initializations. With extensive experimental validation on multiple architectures and tasks, we show that MetaPerturb trained on a single source task and architecture significantly improves the generalization of unseen architectures on unseen tasks, largely outperforming advanced regularization techniques and fine-tuning. MetaPerturb is highly practical as it requires negligible increase in the parameter size, with no adaptation cost and hyperparameter tuning. We believe that with such effectiveness, versatility and practicality, our regularizer has a potential to become a standard tool for regularization.

Broader Impact

Our MetaPerturb regularizer effectively eliminates the need for retraining of the source task because it can generalize to any convolutional neural architectures and to any image datasets. This versatility is extremely helpful for lowering the energy consumption and training time required in transfer learning, because in real world there exists extremely diverse learning scenarios that we have to deal with. Previous transfer learning or meta-learning methods have not been flexible and versatile enough to solve those diverse large-scale problems simultaneously, but our model can efficiently improve the performance with a single meta-learned regularizer. Also, MetaPerturb efficiently extends the previous meta-learning to standard learning frameworks by avoiding the expensive bi-level optimization, which reduces the computational cost of meta-training, which will result in further reduction in the energy consumption and training time.

Acknowledgments and Disclosure of Funding

This work was supported by Google AI Focused Research Award, the Engineering Research Center Program through the National Research Foundation of Korea (NRF) funded by the Korean Government MSIT (NRF-2018R1A5A1059921), and the Institute of Information & communications Technology Planning & Evaluation (IITP) grant funded by the Korea government(MSIT) (No.2019-0-00075, Artificial Intelligence Graduate School Program(KAIST))

References

- [1] A. Achille and S. Soatto. Information dropout: Learning optimal representations through noisy computation. *IEEE transactions on pattern analysis and machine intelligence*, 40(12):2897–2905, 2018.
- [2] A. A. Alemi, I. Fischer, J. V. Dillon, and K. Murphy. Deep variational information bottleneck. 2016.
- [3] M. Andrychowicz, M. Denil, S. Gomez, M. W. Hoffman, D. Pfau, T. Schaul, B. Shillingford, and N. De Freitas. Learning to learn by gradient descent by gradient descent. *Advances in neural information processing systems*, 29, 2016.
- [4] A. Athalye, N. Carlini, and D. Wagner. Obfuscated gradients give a false sense of security: Circumventing defenses to adversarial examples. In *International conference on machine learning*, pages 274–283. PMLR, 2018.
- [5] Y. Balaji, S. Sankaranarayanan, and R. Chellappa. Metareg: Towards domain generalization using meta-regularization. *Advances in neural information processing systems*, 31, 2018.
- [6] A. Coates, A. Ng, and H. Lee. An analysis of single-layer networks in unsupervised feature learning. In *Proceedings of the fourteenth international conference on artificial intelligence and statistics*, pages 215–223. JMLR Workshop and Conference Proceedings, 2011.
- [7] J. Devlin, M.-W. Chang, K. Lee, and K. Toutanova. BERT: Pre-training of deep bidirectional transformers for language understanding. In *Proceedings of the 2019 Conference of the North American Chapter of the Association for Computational Linguistics: Human Language Technologies, Volume 1 (Long and Short Papers)*, pages 4171–4186, Minneapolis, Minnesota, June 2019. Association for Computational Linguistics.
- [8] C. Finn, P. Abbeel, and S. Levine. Model-agnostic meta-learning for fast adaptation of deep networks. In *International conference on machine learning*, pages 1126–1135. PMLR, 2017.
- [9] S. Flennerhag, P. G. Moreno, N. D. Lawrence, and A. Damianou. Transferring knowledge across learning processes. In *International Conference on Learning Representations*, 2018.
- [10] G. Ghiasi, T.-Y. Lin, and Q. V. Le. Dropblock: A regularization method for convolutional networks. volume 31, 2018.
- [11] R. Girshick, J. Donahue, T. Darrell, and J. Malik. Rich feature hierarchies for accurate object detection and semantic segmentation. In *Proceedings of the IEEE conference on computer vision and pattern recognition*, pages 580–587, 2014.
- [12] K. He, X. Zhang, S. Ren, and J. Sun. Deep residual learning for image recognition. In *Proceedings of the IEEE conference on computer vision and pattern recognition*, pages 770–778, 2016.

- [13] S. Ioffe and C. Szegedy. Batch normalization: Accelerating deep network training by reducing internal covariate shift. In *International conference on machine learning*, pages 448–456. PMLR, 2015.
- [14] Y. Jang, H. Lee, S. J. Hwang, and J. Shin. Learning what and where to transfer. In *International Conference on Machine Learning*, pages 3030–3039. PMLR, 2019.
- [15] A. Khosla, N. Jayadevaprakash, B. Yao, and F.-F. Li. Novel dataset for fine-grained image categorization: Stanford dogs. In *Proc. CVPR Workshop on Fine-Grained Visual Categorization (FGVC)*, volume 2. Citeseer, 2011.
- [16] J. Krause, M. Stark, J. Deng, and L. Fei-Fei. 3d object representations for fine-grained categorization. In *Proceedings of the IEEE international conference on computer vision workshops*, pages 554–561, 2013.
- [17] A. Krizhevsky. Learning multiple layers of features from tiny images. 2009.
- [18] Y. Le and X. S. Yang. Tiny imagenet visual recognition challenge. 2015.
- [19] H. B. Lee, T. Nam, E. Yang, and S. J. Hwang. Meta dropout: Learning to perturb latent features for generalization. In *International Conference on Learning Representations*, 2019.
- [20] H. Li, Z. Xu, G. Taylor, C. Studer, and T. Goldstein. Visualizing the loss landscape of neural nets. *Advances in neural information processing systems*, 31, 2018.
- [21] Z. Li and D. Hoiem. Learning without forgetting. *IEEE transactions on pattern analysis and machine intelligence*, 40(12):2935–2947, 2017.
- [22] J. Long, E. Shelhamer, and T. Darrell. Fully convolutional networks for semantic segmentation. In *Proceedings of the IEEE conference on computer vision and pattern recognition*, pages 3431–3440, 2015.
- [23] A. Madry, A. Makelov, L. Schmidt, D. Tsipras, and A. Vladu. Towards deep learning models resistant to adversarial attacks. In *International Conference on Learning Representations*, 2018.
- [24] Z. Mai, G. Hu, D. Chen, F. Shen, and H. T. Shen. Metamixup: Learning adaptive interpolation policy of mixup with metalearning. *IEEE Transactions on Neural Networks and Learning Systems*, 2021.
- [25] S. Maji, E. Rahtu, J. Kannala, M. Blaschko, and A. Vedaldi. Fine-grained visual classification of aircraft. *arXiv preprint arXiv:1306.5151*, 2013.
- [26] M. P. Naeini, G. Cooper, and M. Hauskrecht. Obtaining well calibrated probabilities using bayesian binning. In *Twenty-Ninth AAAI Conference on Artificial Intelligence*, 2015.
- [27] Y. Netzer, T. Wang, A. Coates, A. Bissacco, B. Wu, and A. Y. Ng. Reading digits in natural images with unsupervised feature learning. 2011.
- [28] B. Neyshabur, S. Bhojanapalli, D. McAllester, and N. Srebro. Exploring generalization in deep learning. *Advances in neural information processing systems*, 30, 2017.
- [29] A. Nichol, J. Achiam, and J. Schulman. On first-order meta-learning algorithms. *arXiv preprint arXiv:1803.02999*, 2018.
- [30] E. Perez, F. Strub, H. De Vries, V. Dumoulin, and A. Courville. Film: Visual reasoning with a general conditioning layer. In *Proceedings of the AAAI Conference on Artificial Intelligence*, volume 32, 2018.
- [31] A. Rajeswaran, C. Finn, S. M. Kakade, and S. Levine. Meta-learning with implicit gradients. *Advances in neural information processing systems*, 32, 2019.
- [32] M. Ren, W. Zeng, B. Yang, and R. Urtasun. Learning to reweight examples for robust deep learning. In *International conference on machine learning*, pages 4334–4343. PMLR, 2018.
- [33] O. Russakovsky, J. Deng, H. Su, J. Krause, S. Satheesh, S. Ma, Z. Huang, A. Karpathy, A. Khosla, M. Bernstein, et al. Imagenet large scale visual recognition challenge. *International journal of computer vision*, 115(3):211–252, 2015.
- [34] A. Sharif Razavian, H. Azizpour, J. Sullivan, and S. Carlsson. Cnn features off-the-shelf: an astounding baseline for recognition. In *Proceedings of the IEEE conference on computer vision and pattern recognition workshops*, pages 806–813, 2014.
- [35] J. Shu, Q. Xie, L. Yi, Q. Zhao, S. Zhou, Z. Xu, and D. Meng. Meta-weight-net: Learning an explicit mapping for sample weighting. *Advances in neural information processing systems*, 32, 2019.

- [36] K. Simonyan, A. Vedaldi, and A. Zisserman. Deep inside convolutional networks: Visualising image classification models and saliency maps. *arXiv preprint arXiv:1312.6034*, 2013.
- [37] K. Simonyan and A. Zisserman. Very deep convolutional networks for large-scale image recognition. In *International Conference on Learning Representations*, 2014.
- [38] N. Srivastava, G. Hinton, A. Krizhevsky, I. Sutskever, and R. Salakhutdinov. Dropout: a simple way to prevent neural networks from overfitting. *The journal of machine learning research*, 15(1):1929–1958, 2014.
- [39] C. Tan, F. Sun, T. Kong, W. Zhang, C. Yang, and C. Liu. A survey on deep transfer learning. In *International conference on artificial neural networks*, pages 270–279. Springer, 2018.
- [40] N. Tishby, F. C. Pereira, and W. Bialek. The information bottleneck method. *arXiv preprint physics/0004057*, 2000.
- [41] D. Ulyanov, A. Vedaldi, and V. Lempitsky. Instance normalization: The missing ingredient for fast stylization. *arXiv preprint arXiv:1607.08022*, 2016.
- [42] V. Verma, A. Lamb, C. Beckham, A. Najafi, I. Mitliagkas, D. Lopez-Paz, and Y. Bengio. Manifold mixup: Better representations by interpolating hidden states. In *International Conference on Machine Learning*, pages 6438–6447. PMLR, 2019.
- [43] O. Vinyals, C. Blundell, T. Lillicrap, D. Wierstra, et al. Matching networks for one shot learning. *Advances in neural information processing systems*, 29, 2016.
- [44] C. Wah, S. Branson, P. Welinder, P. Perona, and S. Belongie. The caltech-ucsd birds-200-2011 dataset. 2011.
- [45] Y. Wu and K. He. Group normalization. In *Proceedings of the European conference on computer vision (ECCV)*, pages 3–19, 2018.
- [46] J. Yosinski, J. Clune, Y. Bengio, and H. Lipson. How transferable are features in deep neural networks? *Advances in neural information processing systems*, 27, 2014.
- [47] S. Zagoruyko and N. Komodakis. Paying more attention to attention: Improving the performance of convolutional neural networks via attention transfer. 2016.
- [48] S. Zagoruyko and N. Komodakis. Wide residual networks. In *British Machine Vision Conference 2016*. British Machine Vision Association, 2016.
- [49] M. Zaheer, S. Kottur, S. Ravanbakhsh, B. Póczos, R. R. Salakhutdinov, and A. J. Smola. Deep sets. *Advances in neural information processing systems*, 30, 2017.
- [50] H. Zhang, M. Cisse, Y. N. Dauphin, and D. Lopez-Paz. mixup: Beyond empirical risk minimization. In *International Conference on Learning Representations*, 2018.

Supplementary file for MetaPerturb: Transferable Regularizer for Heterogeneous Tasks and Architectures

Organization The supplementary file is organized as follows. In section A, we show additional results and analysis of the robustness and calibration experiments. In section B, we visualize how the perturbations look like in the latent feature space. In section C, we provide the details of the datasets, network architectures, and experimental setups.

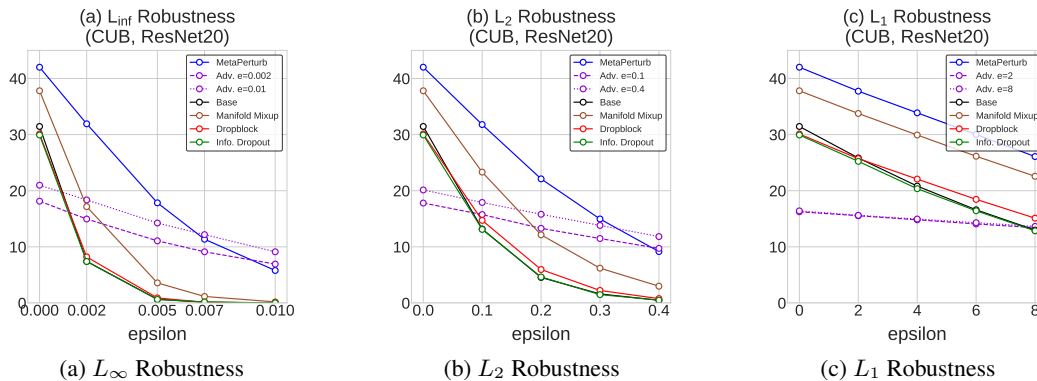


Figure 1: **Adversarial robustness** against PGD attack [12] with varying size of radius ϵ using CUB dataset and ResNet20.

A More Results and Analysis on Robustness and Calibration

Robustness In Figure 1 and Figure 6 in the paper, we measure the adversarial robustness of other baseline regularizers such as Manifold Mixup [18], Dropblock [5], and Information Dropout [2]. We use EoT [3] + PGD attack of 200 steps with some range of ϵ and the inner-learning rate is set to 0.025ϵ for ℓ_∞ and ℓ_2 attack and 0.033ϵ for ℓ_1 attack. For EoT attack, we sample gradients 10 times. We also compare with *adversarial training* baselines, which take 30 projected gradient descent steps at training. The ϵ value used for adversarial training for each dataset is written in the Figure 1 and Figure 6 in the paper. We can see that whereas adversarial training is beneficial for the adversarial accuracies, it largely degrades the clean accuracies. On the other hand, our MetaPerturb regularizer improves both clean accuracy and adversarial robustness than the base model, even without explicit adversarial training.

Calibration In the main paper, we showed that the predictions with MetaPerturb regularizer are better calibrated than those of the baselines. In this section, we provide more results and analysis of calibration on various datasets. First of all, calibration performance is frequently quantified with Expected Calibration Error (ECE) [14]. ECE is computed by dividing the confidence values into multiple bins and averaging the gap between the actual accuracy and the confidence value over all the

Table 1: **ECE of multiple datasets.** Source and target network are ResNet20. TIN: Tiny ImageNet.

Model	# Transfer params	Source dataset	Target Dataset					
			STL10	s-CIFAR100	Dogs	Cars	Aircraft	CUB
Base	0	None	23.36±1.10	33.09±0.50	8.40±0.66	9.78±0.72	10.37±0.92	21.77±0.80
Finetuning	.3M	TIN	15.68±0.40	29.78±0.33	11.41±0.18	7.00±0.84	8.04±0.65	23.05±0.31
Info. Dropout [2]	0	None	22.87±0.28	32.78±0.21	8.27±0.80	8.84±0.77	9.99±1.15	20.41±0.34
DropBlock [5]	0	None	19.65±0.50	28.70±0.17	5.89±0.71	5.83±1.02	7.26±1.55	18.64±0.40
Manifold Mixup [18]	0	None	5.41±0.25	2.26±0.52	5.82±0.42	17.00±0.79	19.80±0.45	9.95±0.50
MetaPerturb	82	TIN	4.80±0.63	14.41±0.65	2.05±0.31	2.82±0.46	2.96±0.37	15.62±1.10

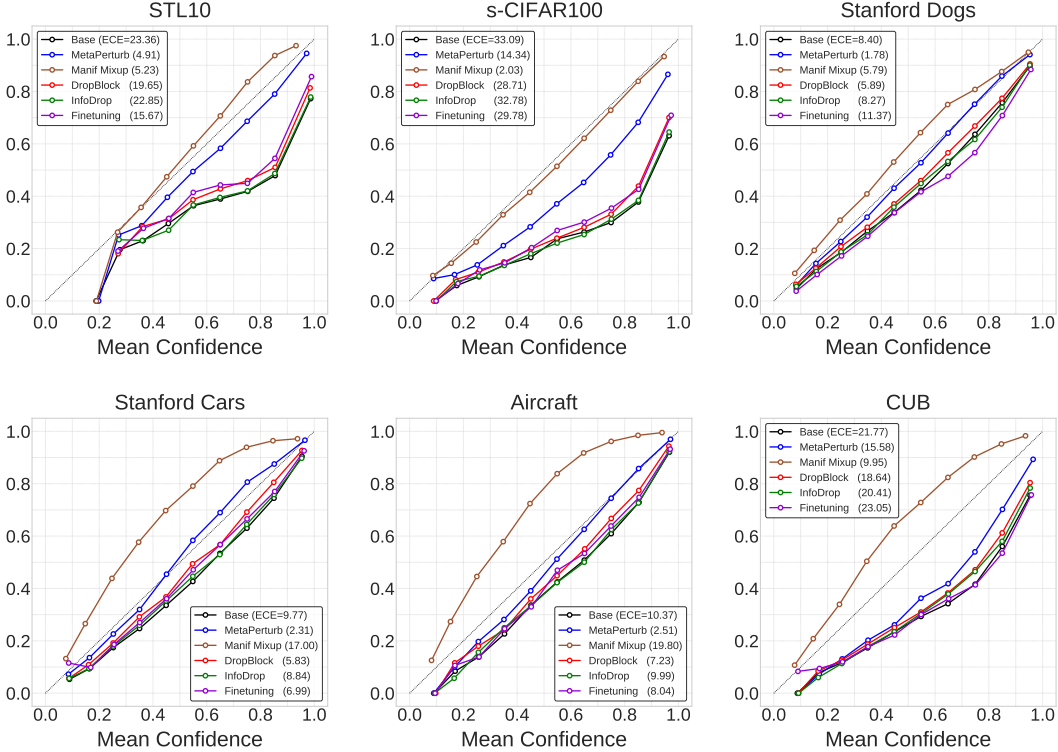


Figure 2: **Calibration plot** on STL10, s-CIFAR100, Stanford Dogs, Stanford Cars, Aircraft and CUB datasets using ResNet20.

bins. Formally, it is defined as

$$\text{ECE} = \mathbb{E}_{\text{confidence}} \left[|p(\text{correct}|\text{confidence}) - \text{confidence}| \right]. \quad (1)$$

Table 1 and Figure 2 show that MetaPerturb produces better-calibrated confidence scores than the baselines on most of the datasets. We conjecture that it is because the parameter of the perturbation function has been meta-learned to lower the negative log-likelihood (NLL) of the test set, similarly to temperature scaling [6] or other popular calibration methods. In other words, we argue that the learning objective of meta-learning is inherently good for calibration by learning to lower the test NLL.

B Visualizations of Perturbation Function

In this section, we visualize the feature maps before and after passing the perturbation function from various datasets. We use ResNet20 network for visualization. We visualize the feature maps from the top to bottom layers in order to see the different levels of layers. Although it is not very straightforward to interpret the results, we can roughly observe that the activation strengths are suppressed by the scale s , and see how the stochastic noise \mathbf{z} transforms the original feature maps.

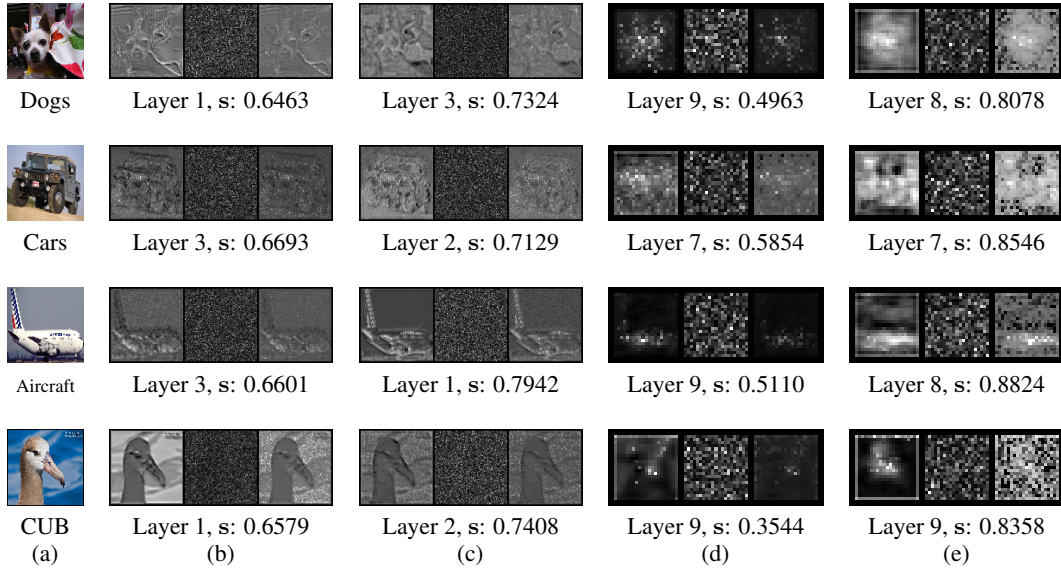


Figure 3: (a) Original image (b-e) **Left:** feature map before passing the perturbation **Center:** generated noise **Right:** feature map after passing the perturbation.

C Experimental Setup

C.1 Meta-training Dataset

Tiny ImageNet This dataset [1] is a subset of ImageNet [16] dataset, consisting of 64×64 size images from 200 classes. There are 500, 50, and 50 images for training, validation, and test dataset, respectively. We use the training dataset for the source training, by resizing images to 32×32 size and dividing dataset into 10 class-wise splits to produce heterogeneous task samples.

C.2 Meta-testing Datasets

STL10 This dataset [4] consists of 10 classes of general objects such as *airplane*, *bird*, and *car*, which is similar to CIFAR-10 dataset but has higher resolution of 96×96 . There are 500 and 800 examples per class for training and test set, respectively. We resized the images to 32×32 size.

small CIFAR-100 This dataset [11] consists of 100 classes of general objects such as *beaver*, *aquarium fish*, and *cloud*. The image size is 32×32 and there are 500 and 100 examples for training and test set, respectively. In order to demonstrate that our model performs well on small dataset, we randomly sample 50 instances per each class from the whole training set and use this smaller set for meta-testing.

Stanford Dogs This dataset [8] is for fine-grained image categorization and contains 20,580 images from 120 breeds of dogs from around the world. It has total 12,000 and 8,580 images for training and testing, respectively. We resized the images to 84×84 size.

Stanford Cars This dataset [10] is also for fine-grained classification, classifying between the Makes, Models, Years of various cars, e.g. 2012 Tesla Model S or 2012 BMW M3 coupe. It contains 16,185 images from 196 classes of cars, where 8,144 and 8,041 images are assigned for training and test set, respectively. We resized the images to 84×84 size.

Aircraft This dataset [13] consists of 10,200 images from 102 different aircraft model variants (most of them are airplane). There are 100 images for each class and we use 6,667 examples for training and 3,333 examples for testing. We resized the images to 84×84 size.

CUB This dataset [20] consists of 200 bird classes such as *Black Tern*, *Blue Jay*, and *Palm Warbler*. It has 5,994 training images and 5,794 test images, and we did not use bounding box information for our experiments. We resized the images to 84×84 size.

small SVHN (s-SVHN) The original dataset [15] consists of 26,032 color images from 10 digit classes. The image size is 32×32 . In our experiments, we randomly sample 500 instances per each class from the whole training set for training in order to simulate data scarce scenario. There are 73,257 examples for testing.

C.3 Networks

We use 6 networks (Conv4 [19], Conv6, VGG9 [17], ResNet20 [7], ResNet44, and Wide ResNet 28-2 [21]) in our experiments. For Conv4, Conv6, and VGG9, we add our perturbation function in every convolution blocks, before activation. For ResNet architectures, we add our perturbation function in every residual blocks, before last activation.

To simply describe the networks, let C_k denote a sequence of a 3×3 convolutional layer with k channels - batch normalization - ReLU activation, M denote a max pooling with a stride of 2, and FC denote a fully-connected layer. We provide a implementation of the networks in our code.

Conv4 This network is frequently used in few-shot classification literature. This model can be described with $C_{64}-M-C_{64}-M-C_{64}-M-C_{64}-M-FC$.

Conv6 This network is similar to the Conv4 network, except that we increase the depth by adding two more convolutional layers. This model can be described with $C_{64}-M-C_{64}-M-C_{64}-M-C_{64}-M-C_{64}-M-FC$.

VGG9 This network is a small version of VGG [17] with a single fully-connected layer at the last. This model can be described with $C_{64}-M-C_{128}-M-C_{256}-M-C_{256}-M-C_{512}-M-C_{512}-M-C_{512}-M-FC$.

ResNet20 This network is used for CIFAR-10 classification task in [7]. The network consists of 3 residual block layers that consist of multiple residual blocks, where each residual block consists of two 3×3 convolution layers. Down-sampling is performed by stride pooling in the first convolution layer in a residual block layer and is used at the second and the third residual block layers. Let $ResBlk(n, k)$ denote a residual block layer with n residual blocks of channel k , and GAP denote a global average pooling. Then, the network can be described with $C_{16}-ResBlk(3, 16)-ResBlk(3, 32)-ResBlk(3, 64)-GAP-FC$.

ResNet44 This network is similar to the ResNet20 network, but with more residual blocks in each residual block layer. The network can be described with $C_{16}-ResBlk(7, 16)-ResBlk(7, 32)-ResBlk(7, 64)-GAP-FC$.

Wide ResNet 28-2 This network is a variant of ResNet, which decrease the depth and increase the width of conventional ResNet architecture. We use Wide ResNet 28-2 which has depth $d = 28$ and widening factor $k = 2$.

C.4 Experimental Details

Meta-training We use an Adam optimizer [9] and train the model for $2K$ steps. We use a learning rate of 10^{-3} . We set the mini-batch size to 512. Lastly, for the base regularizations during training, we use weight decay of 5×10^{-4} and simple data augmentations such as random resizing & cropping and random horizontal flipping. In order to efficiently train multiple tasks, we distribute the tasks to multiple processing units and each process has its own main-model parameters θ and perturbation function parameter ϕ . After one gradient step of the whole model, we share only the perturbation function parameters across the processes.

Meta-testing We use an Adam optimizer [9] and train the model for $10K$ steps. We use an initial learning rate of 10^{-3} and decay the learning rate by 0.3 at $4K$, $7K$, and $9K$ steps. We set the

mini-batch size to 128. The other configurations are as same as the meta-training stage. After the meta-training is done, only the perturbation function parameter ϕ is transferred to the meta-testing stage. Note that ϕ is not updated in the meta-testing stage.

Model selection for transfer learning We empirically observed that ϕ which maximizes the output feature map works well in the meta-test step. Based on this observation, we select the snapshot of the trained MetaPerturb model at the iteration with the largest average feature map value at the penultimate layer. Moreover, since the performance of our perturbation module may vary across multiple meta-training runs due to stochasticity in the initialization and training, we select the best performing model using a validation set, which is comprised of a subset of the CIFAR-100 dataset, with 100 training instances per class. Note that this validation set does not overlap with the s-CIFAR100 we use in the experimental validation. Although the model selection is not entirely necessary, this may be helpful in practice since we observed that a MetaPerturb regularizer with good performance on a specific dataset consistently works well on any datasets.

Code The code is available at <https://github.com/JWoong148/metaperturb>.

References

- [1] <https://tiny-imagenet.herokuapp.com/>.
- [2] A. Achille and S. Soatto. Information Dropout: Learning Optimal Representations Through Noisy Computation. In *TPAMI*, 2018.
- [3] A. Athalye, N. Carlini, and D. Wagner. Obfuscated gradients give a false sense of security: Circumventing defenses to adversarial examples. In *ICML*, 2018.
- [4] A. Coates, A. Ng, and H. Lee. An Analysis of Single-Layer Networks in Unsupervised Feature Learning. In *AISTATS*, 2011.
- [5] G. Ghiasi, T.-Y. Lin, and Q. V. Le. Dropblock: A regularization method for convolutional networks. In *NIPS*, 2018.
- [6] C. Guo, G. Pleiss, Y. Sun, and K. Q. Weinberger. On calibration of modern neural networks. In *ICML*, 2017.
- [7] K. He, X. Zhang, S. Ren, and J. Sun. Deep Residual Learning for Image Recognition. In *CVPR*, 2016.
- [8] A. Khosla, N. Jayadevaprakash, B. Yao, and L. Fei-Fei. Novel dataset for fine-grained image categorization. In *First Workshop on Fine-Grained Visual Categorization, CVPR*, 2011.
- [9] D. P. Kingma and J. Ba. Adam: A method for stochastic optimization. *arXiv preprint arXiv:1412.6980*, 2014.
- [10] J. Krause, M. Stark, J. Deng, and L. Fei-Fei. 3d object representations for fine-grained categorization. In *4th International IEEE Workshop on 3D Representation and Recognition (3dRR-13)*, 2013.
- [11] A. Krizhevsky, G. Hinton, et al. Learning Multiple Layers of features from Tiny Images. *University of Toronto*, 2009.
- [12] A. Madry, A. Makelov, L. Schmidt, D. Tsipras, and A. Vladu. Towards Deep Learning Models Resistant to Adversarial Attacks. In *ICLR*, 2018.
- [13] S. Maji, E. Rahtu, J. Kannala, M. Blaschko, and A. Vedaldi. Fine-Grained Visual Classification of Aircraft. *arXiv preprint arXiv:1306.5151*, 2013.
- [14] M. P. Naeni, G. Cooper, and M. Hauskrecht. Obtaining well calibrated probabilities using bayesian binning. In *AAAI*, 2015.
- [15] Y. Netzer, T. Wang, A. Coates, A. Bissacco, B. Wu, and A. Y. Ng. Reading Digits in Natural Images with Unsupervised Feature Learning. *NIPS*, 2011.
- [16] O. Russakovsky, J. Deng, H. Su, J. Krause, S. Satheesh, S. Ma, Z. Huang, A. Karpathy, A. Khosla, M. Bernstein, et al. ImageNet Large Scale Visual Recognition Challenge. *IJCV*, 2015.
- [17] K. Simonyan and A. Zisserman. Very Deep Convolutional Networks for Large-Scale Image Recognition. In *ICLR*, 2015.

- [18] V. Verma, A. Lamb, C. Beckham, A. Najafi, I. Mitliagkas, D. Lopez-Paz, and Y. Bengio. Manifold Mixup: Better Representations by Interpolating Hidden States. In *ICML*, 2019.
- [19] O. Vinyals, C. Blundell, T. Lillicrap, D. Wierstra, et al. Matching Networks for One Shot Learning. In *NIPS*, 2016.
- [20] C. Wah, S. Branson, P. Welinder, P. Perona, and S. Belongie. The Caltech-UCSD Birds-200-2011 Dataset. Technical Report CNS-TR-2011-001, California Institute of Technology, 2011.
- [21] S. Zagoruyko and N. Komodakis. Wide Residual Networks. In *BMVC*, 2016.